γ-Cyclodextrin Metal-Organic Framework as a Carrier to Deliver Triptolide for the Treatment of Hepatocellular Carcinoma

Zhe Li
Shanghai University of Traditional Chinese Medicine
Gang Yang
Shanghai 9th Peoples Hospital Affiliated to Shanghai Jiaotong University School of Medicine
Rong Wang
Shanghai 9th Peoples Hospital Affiliated to Shanghai Jiaotong University School of Medicine
Yuanyuan Wang
Shanghai 9th Peoples Hospital Affiliated to Shanghai Jiaotong University School of Medicine
Jing Wang
Shanghai 9th Peoples Hospital Affiliated to Shanghai Jiaotong University School of Medicine
Meng Yang
Shanghai 9th Peoples Hospital Affiliated to Shanghai Jiaotong University School of Medicine
Chunai Gong
Shanghai 9th Peoples Hospital Affiliated to Shanghai Jiaotong University School of Medicine
Yongfang Yuan (nmxyyf@126.com)
Shanghai 9th Peoples Hospital Affiliated to Shanghai Jiaotong University School of Medicine

Nano Express

Keywords: γ-Cyclodextrin metal-organic framework, triptolide, bioavailability, anti-tumor

Posted Date: October 29th, 2020

DOI: https://doi.org/10.21203/rs.3.rs-97854/v1

Version of Record: A version of this preprint was published at Drug Delivery and Translational Research on April 15th, 2021. See the published version at https://doi.org/10.1007/s13346-021-00978-7.

Abstract

Triptolide (TPL) has been employed to treat hepatocellular carcinoma (HCC). However, the poor water-solubility of TPL restrict its applications. Therefore, we prepared TPL loaded cyclodextrin-based metal-organic framework (TPL@CD-MOF) to improve the solubility and bioavailability of TPL, thus enhancing the anti-tumor effect on HCC. The BET surface and the pore size of TPL@CD-MOF were 1134.5 $m^2 \cdot g^{-1}$ and 1.6 nm, respectively. The results of XRD indicated that TPL in TPL@CD-MOF was encapsuled. TPL@CD-MOF showed a slower release than free TPL *in vitro*. Moreover, the CD-MOF improved the cell internalization and bioavailability of TPL. TPL@CD-MOF also showed higher anti-tumor efficacy *in vitro* and *in vivo* compared to free TPL. As a carrier, CD-MOF improved the solubility and bioavailability of TPL. In addition, TPL@CD-MOF exhibited improved anti-tumor effects *in vitro* and *in vivo,* indicating great potential as a carrier for insoluble anti-tumor drugs.

Introduction

Hepatocellular carcinoma (HCC) accounts for the majority of primary liver cancers. Liver cancers are the fourth most common cause of cancer-related mortality worldwide [1]. Surgical resection is still the preferred method for the curative treatment of HCC. However, HCC is usually diagnosed at a late stage with only approximately 15% of HCC patients eligible for operative treatment [2–5]. In addition, the effects of first-line therapies with sorafenib or lenvatinib and second-line therapies with regorafenib, cabozantinib or ramucirumab are not so satisfactory, which reminds us to develop new chemotherapy drugs to improve the efficacy of HCC.

Triptolide (TPL), extracted from *Tripterygium wilfordii*, has a variety of bioactivities, such as antioxidation, anti-inflammation and anti-cancer [6]. For anti-tumor, TPL has been employed in the treatment of leukemia lung cancer, colon cancer and HCC [5, 7–10]. However, the clinical applications of TPL are limited due to its narrow therapeutic window, severe toxicity and poor water-solubility [7, 11]. Drug delivery systems (DDSs) have been widely used to improve solubility of insoluble drugs and reduce drug toxicity [12]. Therefore, it is necessary to develop a new DDS to increase the drug solubility and enhance the therapeutic effects. Among different DDS, γ-Cyclodextrin-based metal-organic framework (γ-CD-MOF) with the characteristics of adjustable structures, high specific surface areas, good biocompatibility and high loading has received much attention in recent years and has been successfully applied in drug delivery [13]. Drugs with poor water-solubility such as oleanolic acid, curcumin, ibuprofen and honokiol have been encapsulated in CD-MOF. The solubilities of the drugs were enhanced and the bioavailabilities were also improved [12, 14–16].

Inspired by the research mentioned above, we have prepared TPL loaded CD-MOF (TPL@CD-MOF) to improve the solubility and bioavailability of TPL, thus enhancing the anti-tumor effect on HCC. We hypothesized that after encapsulating TPL into CD-MOF, the solubility and bioavailability of the drug could be improved. TPL@CD-MOF was characterized by scanning electron microscopy (SEM), nitrogen sorption-desorption experiment and X-ray diffraction (XRD). Drug loading, *in vitro* release profile, cell-

uptake study and in *vitro* cytotoxicity of TPL@CD-MOF were tested. Moreover, *in vivo* pharmacokinetics and pharmacodynamics were also investigated.

Materials And Methods

Materials, cell culture, and animals

TPL (purity ≥ 98%) was obtained from Shanghai Yuanye Biotech Co., Ltd. (Shanghai, China). Coumarin-6 (C6) and pharmaceutical grade γ-CD were supplied by Sigma-Aldrich Co. (St.Louis, MO, USA). Potassium hydroxide, methanol, ethanol, polyethylene glycol 20000 (PEG 20000), and other reagents with analytical grade were purchased from Sinopharm Chemical Reagent Co., Ltd. (Shanghai, China). Cell counting kit-8 (CCK-8) was obtained from Beyotime Biotechnology (Shanghai, China). Fetal bovine serum (FBS) and Dulbecco's modified Eagle's medium (DMEM) were obtained from Gibco Inc. (Grand Island, NY, USA). TUNEL apoptosis assay kit was obtained from Roche Pharmaceutical Co., Ltd. (Basel, Switzerland). All other chemicals used were of analytical grade.

The Huh-7 cell line and Caco-2 cell line were purchased from the Cell Bank of Typical Culture Preservation Committee of the Chinese Academy of Sciences (Shanghai, China). Huh-7 cells and Caco-2 cells were cultured in DMEM supplemented with 10% FBS, 1% penicillin/streptomycin in a humidified incubator with 5% CO_2 at 37 °C.

Healthy male Sprague–Dawley (SD) mice (200 ± 20 g) and Balb/c-nu mice (18 ± 2 g) were randomly assigned to different groups. The experiment was approved by the Ethics Committee of Ninth People's Hospital, affiliated with Shanghai Jiao Tong University School of Medicine before the research.

High-performance liquid chromatography (HPLC) analysis

The detection of TPL was performed on a Waters e2695 HPLC system (Waters Technologies, USA) with an Agilent TC-C18 column (250mm × 4.6 mm, 5 μm) and acetonitrile:water = 70:30 as the eluent. The flow rate was set at 1.0 mL·min^{-1} and the column temperature was set at 30 °C. The detection wavelength was 218 nm with an injection volume of 20 μL.

Synthesis and activation of CD-MOF

The CD-MOF was synthesized according to the previously published protocols [16]. Briefly, γ-CD (3.24 g) and potassium hydroxide (1.12 g) were dissolved in 100 mL distilled water with a 20 min incubation at 50 ℃. Then, the obtained solution was mixed with 60 mL methanol. Thereafter, 160 mL PEG20000 methanolic solution (8 mg·mL^{-1}) was added and the solution was kept in cold water for about 12 h to collect the precipitates. To remove the residual potassium hydroxide, γ-CD, and PEG20000, the precipitates were washed 3 times with ethanol (60 mL). To activate the obtained CD-MOF, the precipitates were immersed in dichloromethane for 72 h (refreshing dichloromethane every 24 h). At last, the blank CD-MOF was obtained by centrifugation and dried under vacuum at 50 ℃ overnight.

Drug-Loading

As shown in Fig. 1, TPL was loaded into CD-MOF with solvent adsorption method [17]: 80 mg TPL was dissolved in 2 mL acetonitrile under ultrasonication. 20 mg Blank CD-MOF were then immersed in the TPL solution, stirring for 24 h on a magnetic stirrer (500 rpm) at room temperature. The TPL@CD-MOF was collected by centrifugation, followed by washing 3 times with acetonitrile and drying for 24 h under vacuum at room temperature. C6@CD-MOF was prepared for the cellular uptake study. For C6 loading, 2 mg C6 was dissolved in 2 mL acetonitrile under ultrasonication. Other steps were the same as mentioned above. The loading capacity of TPL was calculated with the following equation [13]:

$$DL = \frac{W_{TPL}}{W_{TPL@CD-MOF}}$$

Where W_{TPL} and $W_{TPL@CD-MOF}$ are weights of TPL and TPL@CD-MOF, respectively.

Characterization

The surface morphology of the blank CD-MOF and TPL@CD-MOF was characterized with a Hitachi S-4800 Scanning Electron Microscopy (SEM) (Tokyo, Japan). The nitrogen adsorption-desorption isotherms of CD-MOF and TPL@CD-MOF at 77 K were determined by a Quadrasorb 2 analyzer. X-ray diffraction (XRD) patterns of the free TPL, physical mixture (PM) and TPL@CD-MOF were conducted on a D8 Advance X-ray diffractometer (Karlsruhe, Germany).

Equilibrium solubility and in vitro release

Solubility of the pure TPL and TPL@CD-MOF was determined in pure water with the published method [13]. In brief, an excess amount of pure TPL or TPL@CD-MOF was added into pure water, shaking (500 rpm) at 25 °C for 72 h to reach the equilibrium. After centrifugation (10000 rpm), the supernatant was analysed by HPLC to measure the concentration of TPL in the solutions.

The *in vitro* release behaviour of the free TPL and TPL@CD-MOF was evaluated. To simulate the fate of TPL@CD-MOF after oral administration, release media with pH 1.2, 7.4 and 6.8 were employed to simulate the gastric fluid, the intestinal fluid and the colonic fluid, respectively. The paddle speed was set at 100 rpm and the temperature was set at 37 ℃. 1 mL release media was then withdrawn at predetermined time points and analyzed by HPLC. In the meantime, 1 mL fresh medium was replenished.

Cell-uptake studies

The cell uptake of C6@CD-MOF by Caco-2 cells was evaluated by a Leica TCS-SP8 confocal laser scanning microscopy (CLSM) (Wetzlar, Germany). 1 mL Caco-2 cells were seeded into confocal dishes at the density of $5 \times 10^4 \cdot mL^{-1}$ 12 h prior to the experiment. Then the culture medium was removed and the cells were washed twice with PBS and incubated with free C6 or C6@CD-MOF solution for 2 h. Thereafter, the cells were rinsed three times with PBS and fixed with 4% paraformaldehyde. After being fixed, the cells

were washed three times with PBS and stained with Hoechst 33258 for 5 min. Finally, the cells were washed three times with PBS again and observed by CLSM.

Cell viability assay

The Cell Counting Kit-8 (CCK-8) was utilized to investigate the cell viability after the treatment with free TPL and TPL@CD-MOF. In brief, 150 μL Huh-7 cells were seeded in 96-well plates at the density of $5 \times 10^4 \cdot mL^{-1}$ overnight. Then, the cells were treated with TPL or TPL@CD-MOF. After treatment for 48 h, 20 μL CCK-8 was added into each well incubating for 2 h. At last, an Infinite M200 PRO microplate reader (Männedorf, Switzerland) was used to assess cell viability by measuring the absorbance at 450 nm.

In vivo pharmacokinetic studies

Ten healthy male SD mice (200 ± 20 g) were randomly divided into two groups with five mice in each group. They were orally administered with free TPL or TPL@CD-MOF at a dose of 1.5 $mg \cdot kg^{-1}$. Blood samples were collected from the retro-orbital plexus into heparinized tubes at predetermined time points centrifuging immediately (3,000 rpm for 10 minutes) to obtain plasma. Then, 0.1 mL plasma was extracted with 1.2 mL ethyl acetate for 3 times. The top organic layers were combined and dried. The residue was redissolved in 0.1 mL of acetonitrile and centrifuged. The supernatant was analyzed by HPLC.

In vivo anti-tumor activity

For establishing xenografts, 2×10^6 Huh-7 cells were injected subcutaneously into the left axillary region of male Balb/c-nu mice [5]. The tumor volumes and weights of the mice were measured every 2 days. When the tumor volume growed up to 50 mm^3 [18], the mice were then randomized to 3 groups and administered by gavage with saline, free TPL or TPL@CD-MOF at a dose of 1.5 $mg \cdot kg^{-1}$ TPL everyday for 10 days. All mice were sacrificed one day after the last administration. The tumors were harvested and weighed, followed by TUNEL and hematoxylin & eosin (H&E) staining assay.

Statistical analysis

Data were expressed as mean ± standard deviation (SD). The pharmacokinetic parameters were analysed with DAS 2.0 software (BioGuider Co, Shanghai, China). All data analysis of variance were performed with the SPSS version 19.0 software (SPSS Inc., Chicago, USA). $P < 0.05$ was considered statistically significant.

Results And Discussion

Preparation and characterization of TPL@CD-MOF

CD-MOF was synthesized with solvothermal method, which was identified as one of the best procedures for the synthesis of CD-MOF. The drug loading of TPL@CD-MOF (28.89%) was significantly higher than that of other TPL loaded nanoparticles [19]. As shown in Fig. 2a, SEM images of the blank CD-MOF and

TPL@CD-MOF indicated that the particles were uniform cubic crystals with a particle size of about 200–500 nm. The nitrogen adsorption-desorption isotherms of the TPL@CD-MOF and blank CD-MOF were shown in Fig. 2b. The BET surface and the pore size of TPL@CD-MOF and blank CD-MOF were 1134.5 $m^2 \cdot g^{-1}$ and 10.4 $m^2 \cdot g^{-1}$, and 1.6 nm and 1.1 nm, respectively. The decrease of the BET surface and the pore size reflected the success of drug loading, which was similar to other drug-loaded CD-MOF [16]. XRD was used to confirm the physical state of TPL in CD-MOF. As shown in Fig. 2c, the free TPL and PM had characteristic diffraction peaks at 2θ = 8.60°, 15.26° and 33.80°. After loading into TPL@CD-MOF, the characteristic peaks of TPL disappeared, which indicated that TPL in TPL@CD-MOF was encapsuled and converted from crystalline state into amorphous state.

Equilibrium solubility and in vitro release

The solubility of drug is a key parameter and determines its bioavailability. The clinical application of TPL has been limited due to its poor solubility [16]. After loading into CD-MOF, the equilibrium solubility of TPL@CD-MOF in pure water reached 308.19 $\mu g \cdot mL^{-1}$, which was about 9.5 times higher than that of free TPL (Fig. 3a). The enhanced solubility of TPL might be attributed to TPL in TPL@CD-MOF transformed from crystalline state into amorphous state, as shown in XRD. *In vitro* drug release of of TPL and TPL@CD-MOF was carried out in release media with pH 1.2, 7.4 and 6.8 (containing 1% sodium dodecyl sulphate solution). In the release media with pH 1.2, the free TPL and TPL@CD-MOF showed a burst release with about 40.00% of the drug released in the first 2 h (Fig. 3b). After an additional 4 h release in the simulated intestinal fluid (pH 7.4), the free TPL and TPL@CD-MOF released 82% and 72%, respectively. For the release in pH 6.8, the cumulative release percentage of both free TPL and TPL@CD-MOF reached about 97% within 12 h. On the whole, TPL@CD-MOF showed a slower release than free TPL, which may be attributed to the drug diffusion being hindered after loading into CD-MOF.

Cell-uptake studies

For cell-uptake studies, Caco-2 cells were adopted to simulate the gastrointestinal (GI) drug barrier for oral delivery [20]. C6 was used as a fluorescent probe to label CD-MOF. As shown in Fig. 4, C6@CD-MOF had a higher green fluorescent signal level in cytoplasm than free C6. The results were in accordance with the previous literature and accounted for a higher diffusion and absorption of C6 into Caco-2 cells [16]. Based on the results, it could be inferred that CD-MOF potentially improved the cell internalization of drugs at the GI level, a previous and necessary step for drugs into the bloodstream.

Cell viability assay

The cytotoxicity of free TPL and TPL@CD-MOF on Huh-7 cells were evaluated by MTT assay. As shown in Fig. 5, a dose-dependent increase in cell death was observed after 48 h of incubation with free TPL or TPL@CD-MOF. The IC_{50} of free TPL and TPL@CD-MOF on Huh-7 cells were 14.02 and 7.80 nM, respectively. The TPL@CD-MOF were found to be more toxic towards Huh-7 cells compared with free TPL, which indicated that the TPL@CD-MOF helped drugs to make use of its

anticancer efficacy.

In vivo pharmacokinetic studies

The plasma concentration-time profiles of TPL after administering intragastrically with free TPL and TPL@CD-MOF in SD rats were shown in Fig. 6. The pharmacokinetic parameters were listed in Table 1. The bioavailability of TPL were significantly improved after loading into CD-MOF with C_{max} and $AUC_{0-\infty}$ of TPL@CD-MOF 1.62- and 1.82-fold improved respectively in comparison with those of the free TPL. Based on the improved bioavailability of TPL and cell-uptake, it could be included that CD-MOF improved the cell internalization of TPL at the GI level and made more TPL absorbed into the bloodstream. The T_{max} for free TPL or TPL@CD-MOF was 0.5 h or 1.2 h, respectively. The longer T_{max} of TPL@CD-MOF could be due to the slower release of TPL compared with that of the free TPL.

Table 1
Main pharmacokinetic parameters of the pure TPL powder and TPL@CD-MOF after oral administration to SD rats at a dose of 1.5 mg·kg^{-1} (n = 5).

Pharmacokinetic parameters	TPL	TPL@CD-MOF
C_{max} (μg·L^{-1})	21.25 ± 2.39	34.35 ± 5.08*
T_{max} (h)	0.50 ± 0.00	1.20 ± 0.45*
$MRT_{0-\infty}$ (h)	41.39 ± 12.58	34.33 ± 11.85
$AUC_{0-\infty}$ (μg·h·L^{-1})	395.84 ± 122.89	721.80 ± 237.66*
[a]Abbreviations: C_{max}, peak plasma concentration; T_{max}, time to reach the peak plasma concentration; $t_{1/2}$, elimination half-life; $AUC_{0-\infty}$, area under the plasma concentration–time curve.		
[b]*: $P \leq 0.05$ compared with the pure TPL powder.		

In vivo anti-tumor activity

Body weights (Fig. 7a) and tumors volumes (Fig. 7b) of the mice were measured every two days after first dose. During the treatment, the weight of the mice in all groups growed slowly. TPL@CD-MOF group showed superior anti-tumor efficacy with smaller tumor size and tumor weight (Fig. 7c and Fig. 7d) when compared with saline or free TPL group. Furthermore, we also evaluated the cell apoptosis in the harvested tumor tissues by H&E and TUNEL staining (Fig. 8). For TUNEL staining, TUNEL positivity (green fluorescence) was barely observed in the excised tumor tissues originated from saline group. However, TUNEL signals were observed in the excised tumor tissues originated from the free TPL group and TPL@CD-MOF group. Additionally, TUNEL signals were highest in TPL@CD-MOF group, which indicated that TPL@CD-MOF induced more apoptosis in tumor tissues when compared with other groups. Similar results were also observed in H&E staining assay. For saline group, tumor tissue displayed minor necrosis, compact structure and dense tumor cells. But various degrees of apoptotic morphological

characteristics, like nuclear pyknosis and karyorrhexis were found in free TPL group and TPL@CD-MOF group, particularly obvious in TPL@CD-MOF group. From the above, TPL@CD-MOF showed better anti-tumor effect *in vivo* compared to other groups, which might be attributed to the improved bioavailability of TPL@CD-MOF.

Conclusion

In this research, we synthesized CD-MOF with solvothermal method, loaded TPL into CD-MOF with solvent adsorption method, and evaluated the bioavailability and anti-tumour effect of TPL@CD-MOF *in vitro* and *in vivo*. CD-MOF with a particle size of about 200-500 nm were obtained. According to the results of nitrogen adsorption-desorption and XRD, we could conclude that TPL was successfully loaded into CD-MOF in an amorphous state. For equilibrium solubility and *in vitro* release, the solubility of TPL was improved in pure water and showed slower release behaviour after loading into CD-MOF. Moreover, the CD-MOF improved the cell internalization of drugs and bioavailability of TPL. TPL@CD-MOF also showed higher anti-tumor efficacy *in vitro* and *in vivo* when compared to free TPL, as shown by the changes in Huh-7 cell viability, tumor volumes, and H&E or TUNEL staining. Therefore, CD-MOF exhibited excellent potential as a carrier for insoluble anti-cancer drugs.

Abbreviations

AUC: Area under the curve; CCK-8: Cell counting kit 8; C6: Coumarin-6; CLSM: Confocal laser scanning microscopy; C_{max}: peak plasma concentration; DAPI: 4',6-diamidino-2-phenylindole; DMEM: Dulbecco's modified Eagle's medium; DDSs: Drug delivery systems; FBS: Fetal bovine serum; GI: Gastrointestinal; H&E: Hematoxylin and eosin; HCC: Hepatocellular carcinoma; PEG 20000: Polyethylene glycol 20000; PM: Physical mixture; SEM: Scanning electron microscopy; SD: Sprague–Dawley; TPL: Triptolide; TPL@CD-MOF: TPL loaded cyclodextrin-based metal-organic framework; T_{max}: time to reach the peak plasma concentration; XRD: X-ray powder diffraction.

Declarations

Acknowledgements

Not applicable.

Authors' contributions

LZ, YG and YY designed and participated equally all the experiments and article writing and should be considered as co-first authors. WR, WY, WJ, YM and GC helped analyze the data and participated in some experiments. All authors have read and approved the final manuscript.

Funding

This work was financially supported by the National Natural Science Foundation of China (No. 81903141, No. 81973275) and Shanghai Sailing Program (No. 20YF1424000).

Availability of data and materials

All data are fully available without restriction.

Competing interests

The authors declared no competing interests.

References

1. Villanueva A. Hepatocellular Carcinoma. *N. Engl. J. Med.* 2019; 380: 1450-1462.
2. Chen H, Wong CC, Liu D, Go M, Wu B, Peng S, et al. APLN promotes hepatocellular carcinoma through activating PI3K/Akt pathway and is a druggable target. *Theranostics.* 2019; 9: 5246-5260.
3. Fares N, Peron JM. Epidemiology, natural history, and risk factors of hepatocellular carcinoma. *Rev. Prat.* 2013; 63: 216-217, 220-222.
4. Zhang X, Liu T, Li Z, Feng Y, Corpe C, Liu S, et al. Hepatomas are exquisitely sensitive to pharmacologic ascorbate (P-AscH(-)). *Theranostics.* 2019; 9: 8109-8126.
5. Alsaied OA, Sangwan V, Banerjee S, Krosch TC, Chugh R, Saluja A, et al. Sorafenib and triptolide as combination therapy for hepatocellular carcinoma. *Surgery.* 2014; 156: 270-279.
6. Li X, Lu Q, Xie W, Wang Y, Wang G. Anti-tumor effects of triptolide on angiogenesis and cell apoptosis in osteosarcoma cells by inducing autophagy via repressing Wnt/beta-Catenin signaling. Biochem *Biophys. Res. Commun.* 2018; 496: 443-449.
7. Chen F, Liu Y, Wang S, Guo X, Shi P, Wang W, et al. Triptolide, a Chinese herbal extract, enhances drug sensitivity of resistant myeloid leukemia cell lines through downregulation of HIF-1alpha and Nrf2. *Pharmacogenomics.* 2013; 14: 1305-1317.
8. Lin C, Zhang X, Chen H, Bian Z, Zhang G, Riaz MK, et al. Dual-ligand modified liposomes provide effective local targeted delivery of lung-cancer drug by antibody and tumor lineage-homing cell-penetrating peptide. *DrugDeliv.* 2018; 25: 256-266.
9. Liu H, Tang L, Li X, Li H. Triptolide inhibits vascular endothelial growth factor-mediated angiogenesis in human breast cancer cells. *Exp. Ther. Med.* 2018; 16: 830-836.
10. Li SG, Shi QW, Yuan LY, Qin LP, Wang Y, Miao YQ, et al. C-Myc-dependent repression of two oncogenic miRNA clusters contributes to triptolide-induced cell death in hepatocellular carcinoma cells. *J. Exp. Clin. Cancer. Res.* 2018; 37: 51.
11. Ling D, Xia H, Park W, Hackett MJ, Song C, Na K, et al. pH-sensitive nanoformulated triptolide as a targeted therapeutic strategy for hepatocellular carcinoma. *ACS Nano.* 2014; 8: 8027-8039.
12. Zhang L, Chen Y, Shi R, Rang T, Pang G, Wang B, et al. Synthesis of hollow nanocages MOF-5 as drug delivery vehicle to solve the load-bearing problem of insoluble antitumor drug oleanolic acid (OA).

Inorg. Chem. Commun. 2018; 96: 20-23.

13. Kritskiy I, Volkova T, Surov A, Terekhova I. gamma-Cyclodextrin-metal organic frameworks as efficient microcontainers for encapsulation of leflunomide and acceleration of its transformation into teriflunomide *Carbohydr. Polym.* 2019; 216: 224-230.
14. Moussa Z, Hmadeh M, Abiad MG, Dib OH, Patra D. Encapsulation of curcumin in cyclodextrin-metal organic frameworks: Dissociation of loaded CD-MOFs enhances stability of curcumin. *Food Chem.* 2016; 212: 485-494.
15. Hartlieb KJ, Ferris DP, Holcroft JM, Kandela I, Stern CL, Nassar MS, et al. Encapsulation of Ibuprofen in CD-MOF and Related Bioavailability Studies. *Mol. Pharm.* 2017; 14: 1831-1839.
16. He Y, Hou X, Guo J, He Z, Guo T, Liu Y, et al. Activation of a gamma-cyclodextrin-based metal-organic framework using supercritical carbon dioxide for high-efficient delivery of honokiol. *Carbohydr. Polym.* 2020; 235: 115935.
17. Chen G, Luo J, Cai M, Qin L, Wang Y, Gao L, et al. Investigation of Metal-Organic Framework-5 (MOF-5) as an Antitumor Drug Oridonin Sustained Release Carrier. *Molecules.* 2019; 24.
18. Bao Y, Yin M, Hu X, Zhuang X, Sun Y, Guo Y, et al. A safe, simple and efficient doxorubicin prodrug hybrid micelle for overcoming tumor multidrug resistance and targeting delivery. *J. Control. Release.* 2016; 235: 182-194.
19. Gu Y, Tang X, Yang M, Yang D, Liu J. Transdermal drug delivery of triptolide-loaded nanostructured lipid carriers: Preparation, pharmacokinetic, and evaluation for rheumatoid arthritis. *Int. J. Pharm.* 2019; 554: 235-244.
20. Duran-Lobato M, Martin-Banderas L, Goncalves LMD, Fernandez-Arevalo M, Almeida AJ. Comparative study of chitosan- and PEG-coated lipid and PLGA nanoparticles as oral delivery systems for cannabinoids. *J. Nanopart. Res.* 2015; 17.

Figures

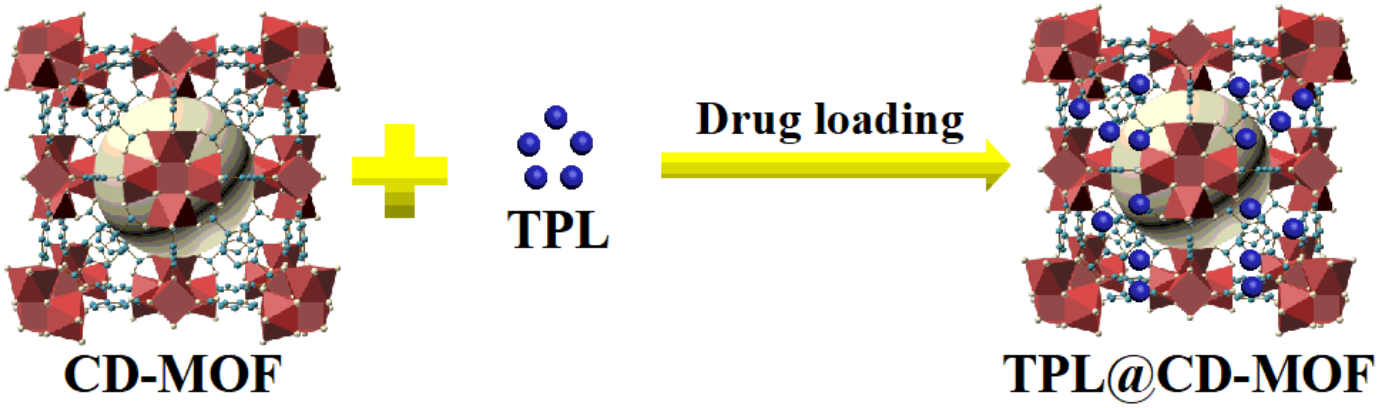

Figure 1

Schematic representation of TPL encapsulated into CD-MOF.

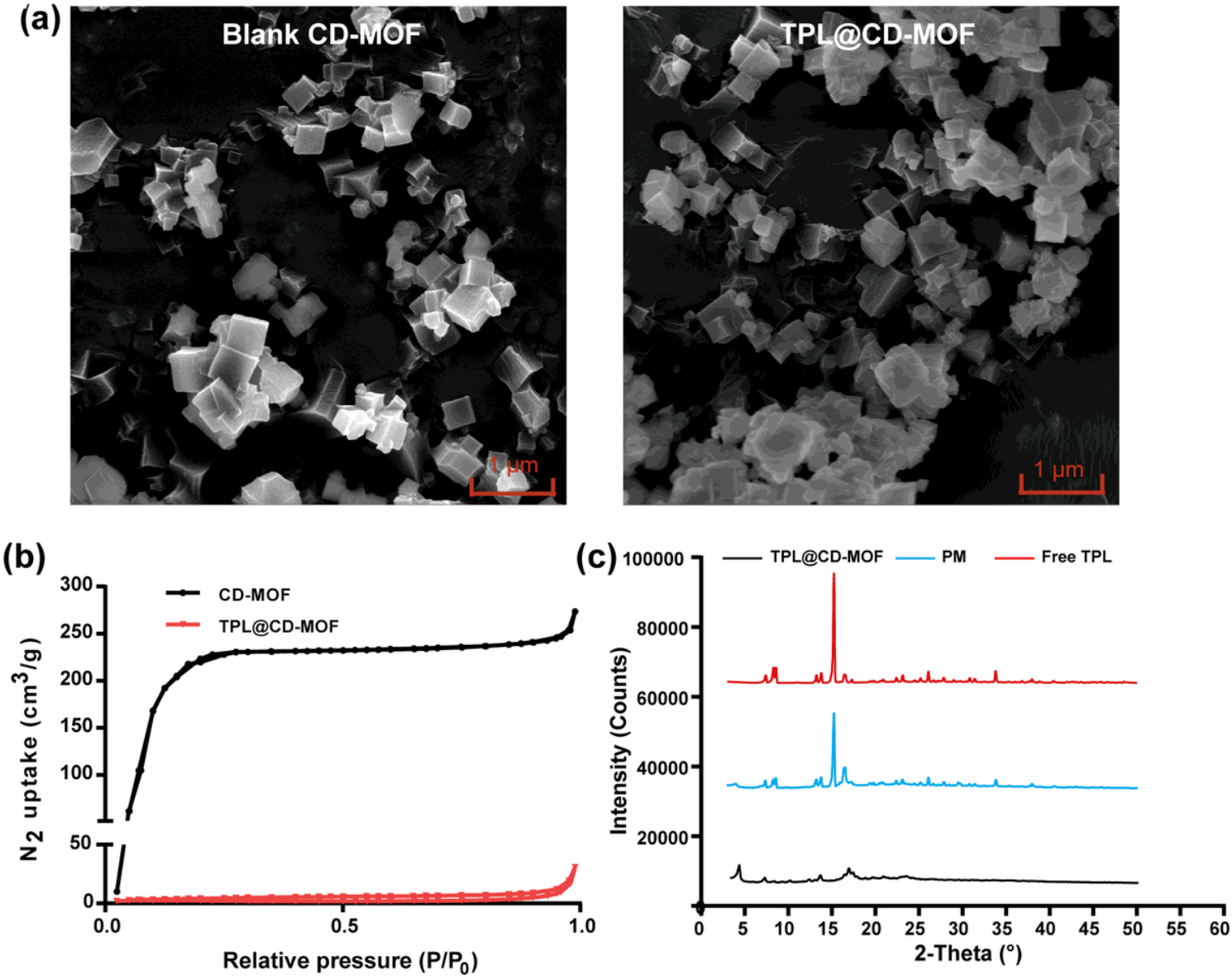

Figure 2

Characterization of TPL@CD-MOF (a) the SEM micrographs of the blank CD-MOF and TPL@CD-MOF; (b) the nitrogen adsorption-desorption isotherms of the blank CD-MOF and TPL@CD-MOF; (c) XRD curves of the free TPL, PM and TPL@CD-MOF.

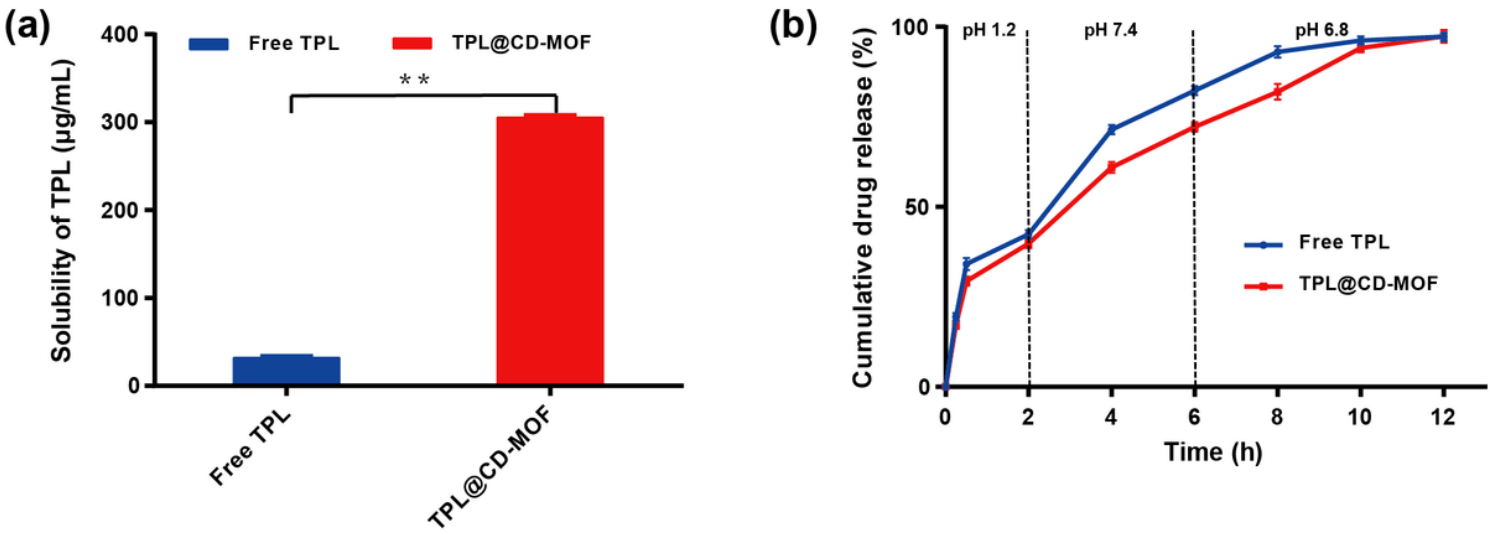

Figure 3

(a) solubility of pure TPL and TPL@CD-MOF in pure water at 25 °C; (b) the in vitro release curves of TPL and TPL@CD-MOF in 1% sodium dodecyl sulphate solution (pH 1.2, 7.4 and 6.8).

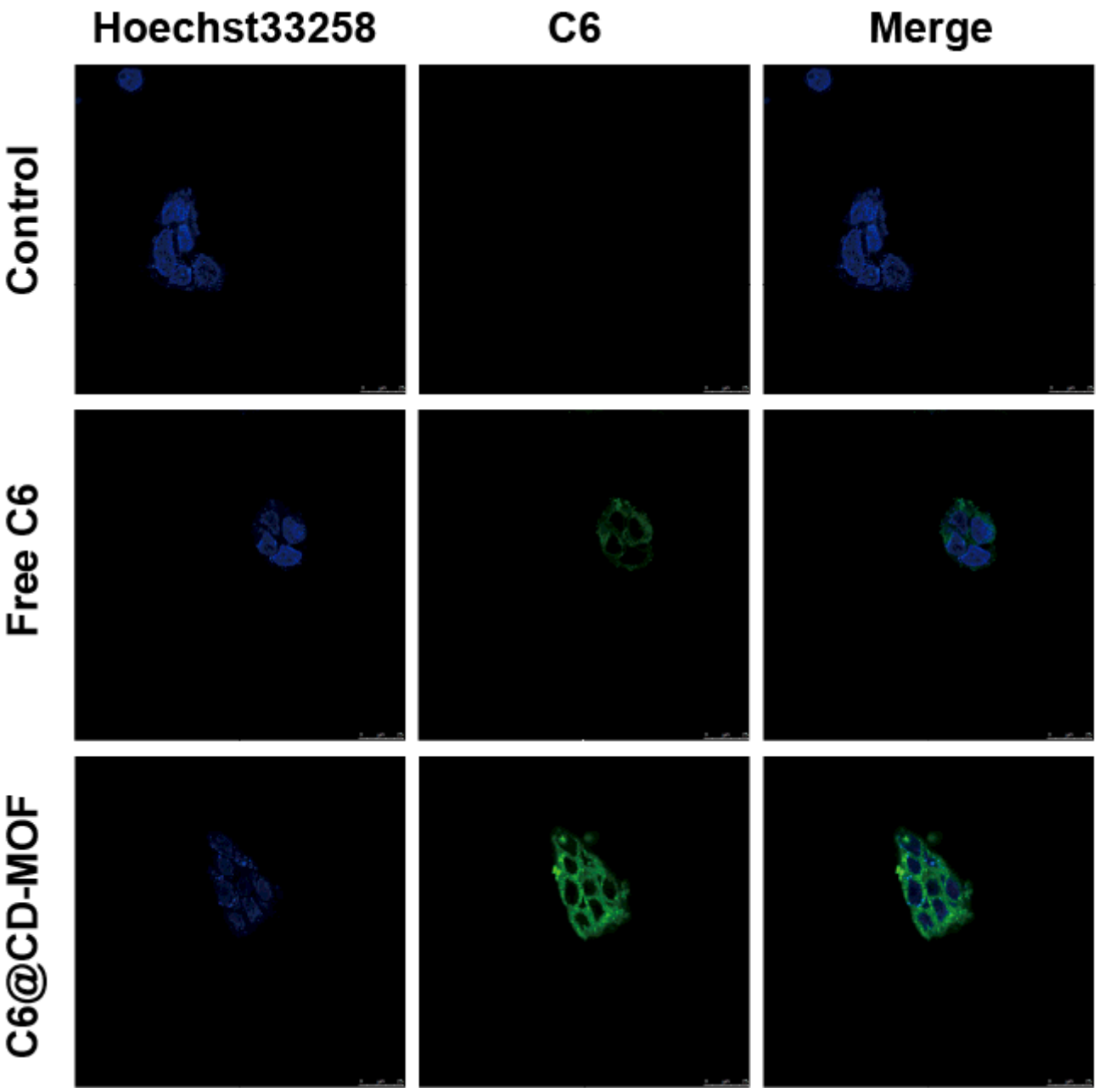

Figure 4

Cellular uptake of C6-labeled CD-MOF by Caco-2 cells after incubation for 2 h.

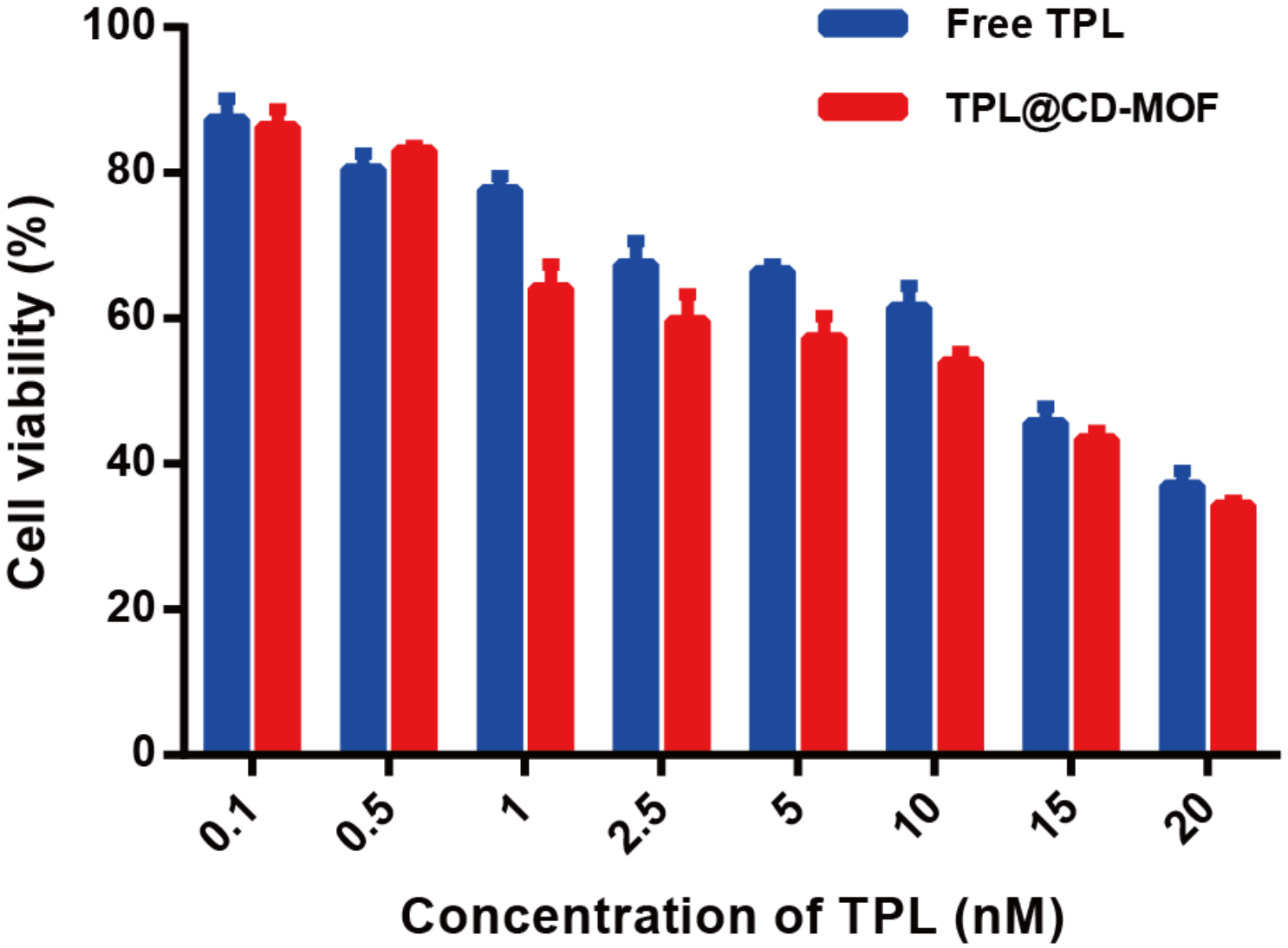

Figure 5

The cytotoxicity of free TPL and TPL@CD-MOF on Huh-7 cells.

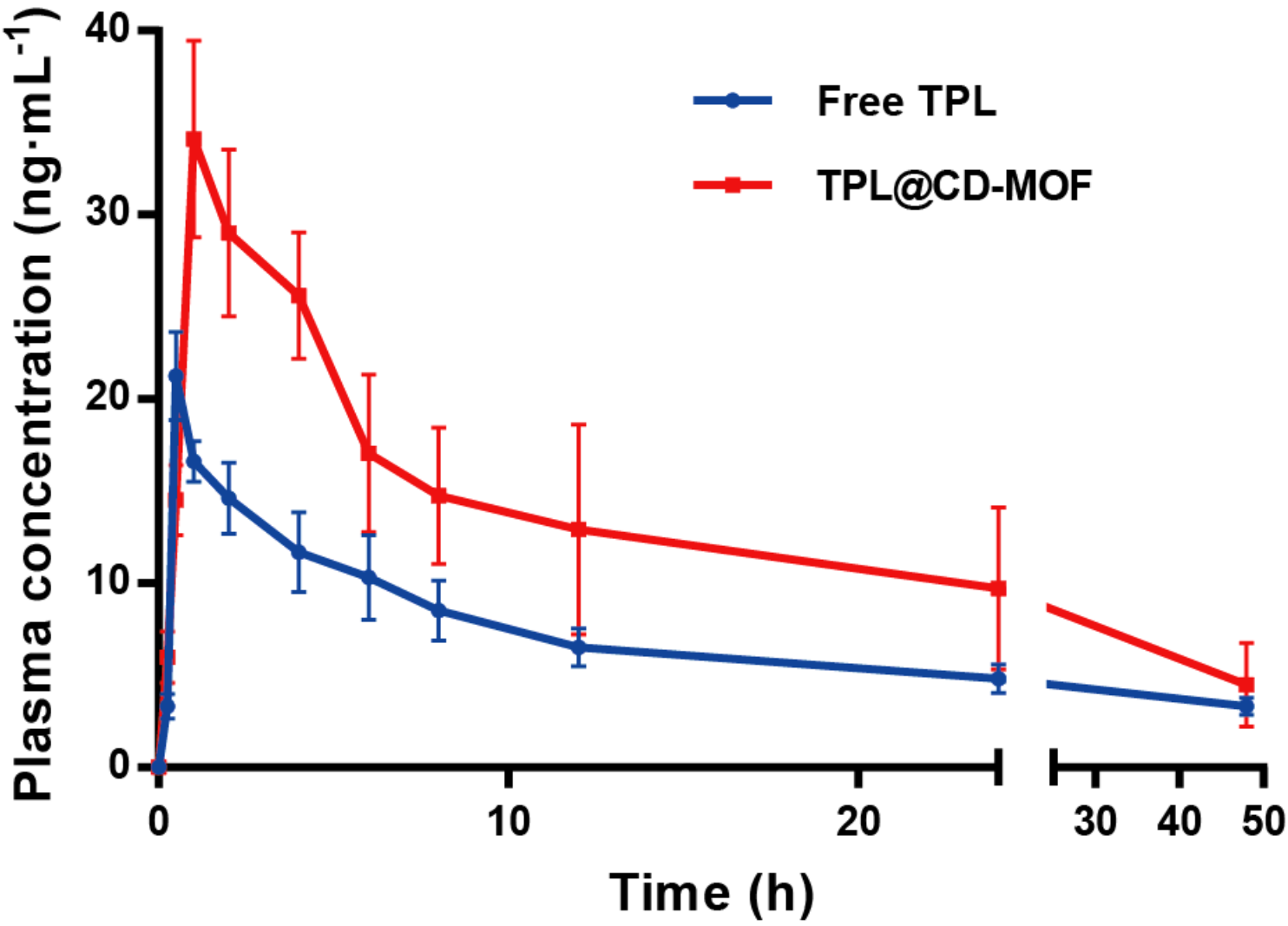

Figure 6

The plasma concentration-time profiles of TPL after single oral administration of test formulations in SD rats (n=5).

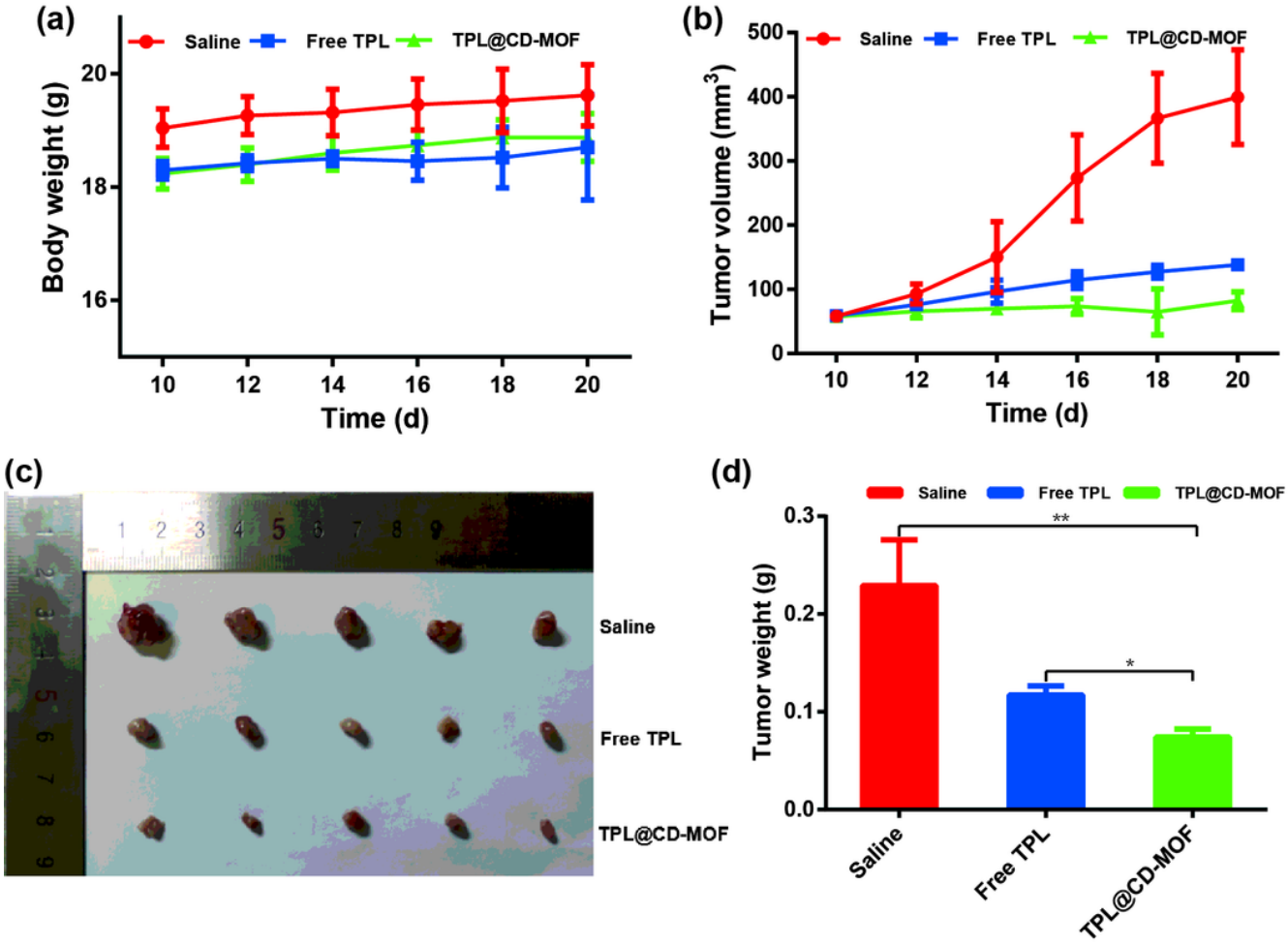

Figure 7

(a) body weights and (b) tumor volumes changes of tumor-bearing Balb/c-nu mice after treated with different formulations (c) photographs of tumors collected from different treatment groups at the end of the treatment (d) tumor weight measured at the end of the treatment (n=5;**P□0.01;*P□0.05).

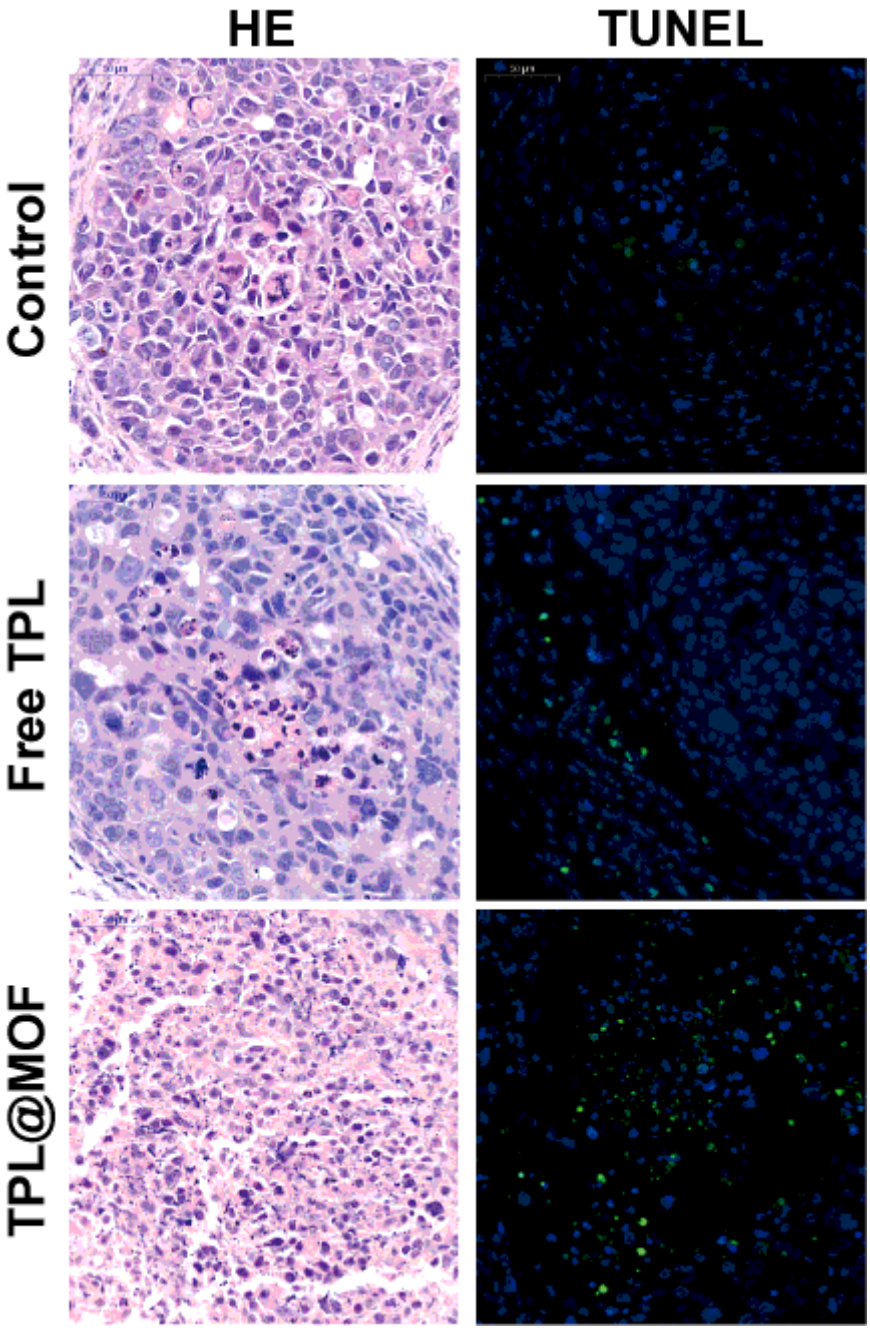

Figure 8

H&E staining and TUNEL staining of the isolated tumor tissue collected from different treatment groups at the end of the treatment.